The American Journal of Human Genetics, Volume *110*

Supplemental information

Rare *de novo* gain-of-function missense variants in *DOT1L* are associated with developmental delay and congenital anomalies

Zelha Nil, Ashish R. Deshwar, Yan Huang, Scott Barish, Xi Zhang, Sanaa Choufani, Polona Le Quesne Stabej, Ian Hayes, Patrick Yap, Chad Haldeman-Englert, Carolyn Wilson, Trine Prescott, Kristian Tveten, Arve Vøllo, Devon Haynes, Patricia G. Wheeler, Jessica Zon, Cheryl Cytrynbaum, Rebekah Jobling, Moira Blyth, Siddharth Banka, Alexandra Afenjar, Cyril Mignot, Florence Robin-Renaldo, Boris Keren, Oguz Kanca, Xiao Mao, Daniel J. Wegner, Kathleen Sisco, Marwan Shinawi, Undiagnosed Disease Network, Michael F. Wangler, Rosanna Weksberg, Shinya Yamamoto, Gregory Costain, and Hugo J. Bellen

SUPPLEMENTAL INFORMATION

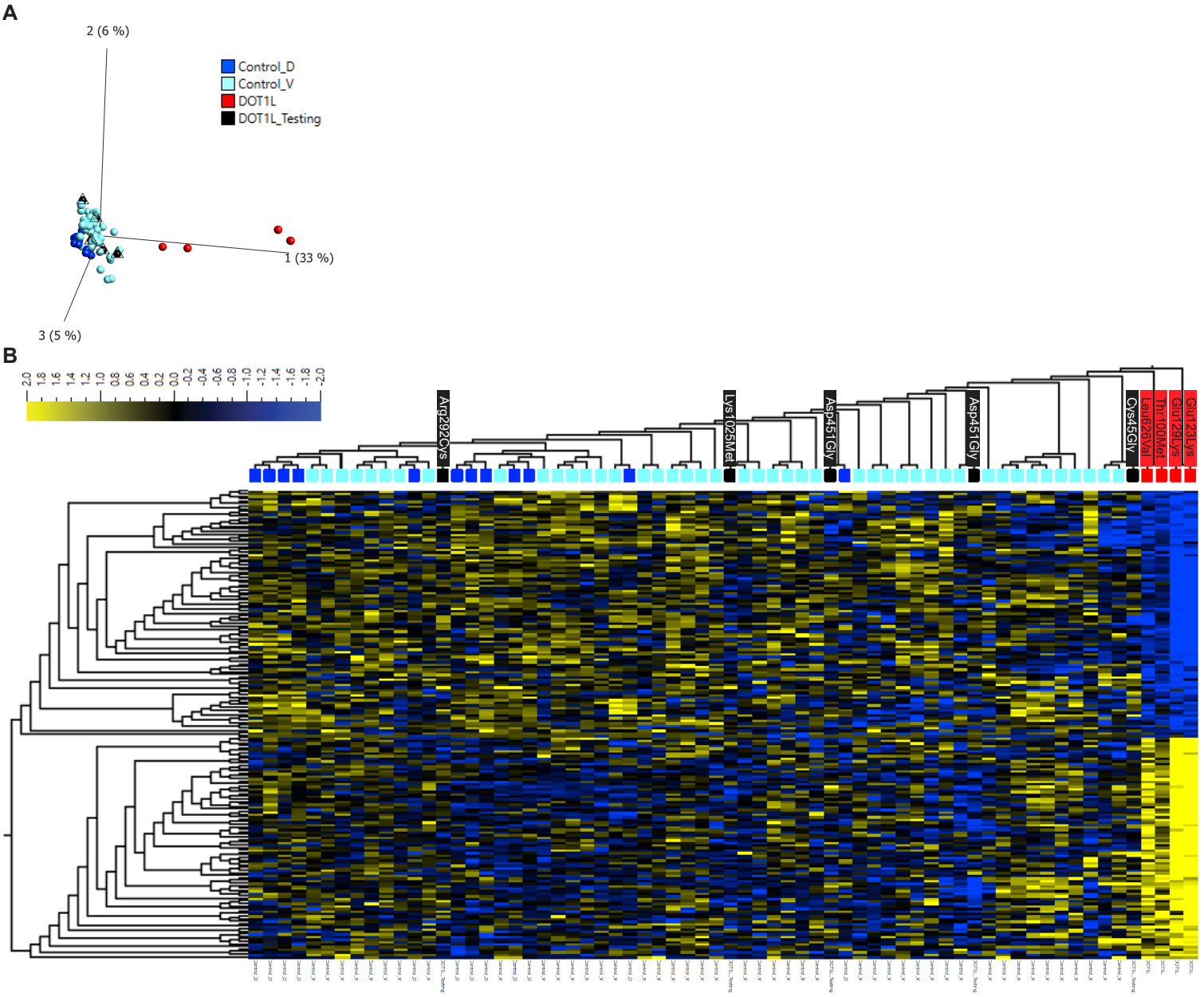

Figure S1. DNA methylation profile of proband blood samples

(A) Principal component analysis (PCA) and (B) heatmap showing clustering of the useable DOT1L samples (red) and matched control samples (blue) using DNAm values at the 185 CpG sites associated with a distinct DOT1L specific DNAm profile. The heatmap color gradient indicates the normalized DNAm value ranging from −2.0 (blue) to 2.0 (yellow). Euclidean distance metric is used in the heatmap clustering dendrograms. Please see Table S9 for significantly enriched CpG sites.

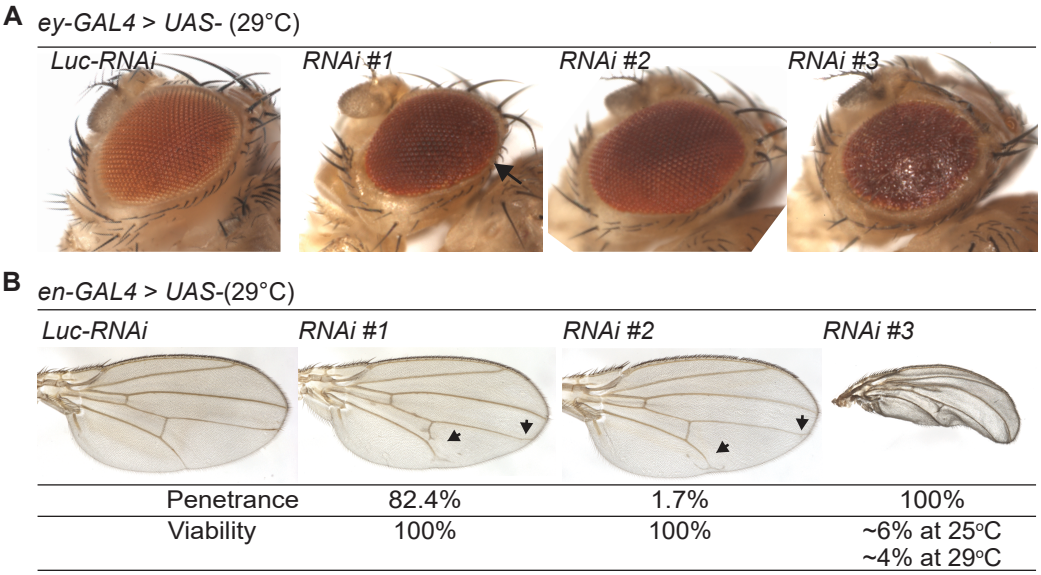

Figure S2. Tissue specific knockdown of gpp causes eye and wing phenotypes

(A) Eye specific knockdown of *gpp* causes a rough eye phenotype. *Ey-GAL4 > gpp-RNAi #1* causes a mild phenotype in a region of the eye indicated with an arrow. *Ey-GAL4 > RNAi #3* causes a severe phenotype in the whole eye. *Ey-GAL4 > RNAi #2* does not cause any phenotype. All the crosses were performed at 29ºC. (ey: eyeless)

(B) Knockdown of *gpp* in developing tissues causes wing phenotypes and lethality. *en-GAL4 > gpp-RNAi #1* causes cross vein branching with a penetrance of 82.4%. *en-GAL4 > RNAi #3* causes lethality and the survivors have a severe phenotype in the whole wing with a full penetrance. *en-GAL4 > RNAi #2* causes vein branching phenotype with a very low penetrance. All the crosses were performed at 29ºC. (en: engrailed)

UAS-DOT1L/+*	gpp^{TG4}/*Df* (18, 25 & 29°C)
*Reference	Lethal
*p.Cys45Gly	Lethal
*p.Thr100Met	Lethal
*p.Glu123Lys	Lethal
*p.Glu129Lys	Lethal
*p.Arg292Cys	Lethal
*p.Leu626Val	Lethal
*p.Lys1025Met	Lethal
GR^{gpp}	Viable

Figure S3. Human reference or variant *DOT1L* fails to rescue lethality

Expression of reference or variant *DOT1L* in gpp^{TG4}/*Df* flies failed to rescue the lethality at all temperatures (18°C, 25°C and 29°C) tested while reintroduction of GR construct fully rescued lethality.

A

$gpp^{TG4/+}$ > *UAS-DOT1L** (25°C)		
	Phenotype	Penetrance
*Reference	wing defects	96.6%
*p.Cys45Gly	wing defects	97.7%
*p.Thr100Met	wing defects	97.3%
*p.Glu123Lys	wing defects	100%
*p.Glu129Lys	wing defects	100%
*p.Arg292Cys	wing defects	98.3%
*p.Leu626Val	wing defects	98.5%
*p.Lys1025Met	wing defects	97.8%

B

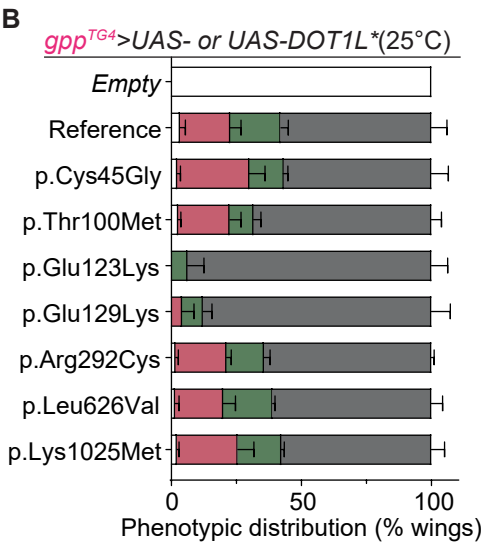

Figure S4. Expression of reference or variant DOT1L in gpp expressing cells causes wing deformities

(A) Survivors of heterozygous mutant flies, $gpp^{TG4/+}$, expressing reference or variant *DOT1L* cDNA show morphological wing defects such as whole wing blistering, necrosis, loss of cross-veins and extra vein branching with penetrance levels >95%.

(B) The distribution of different wing phenotypes in survivors of heterozygous mutant flies, $gpp^{TG4/+}$, expressing each *DOT1L* cDNA.

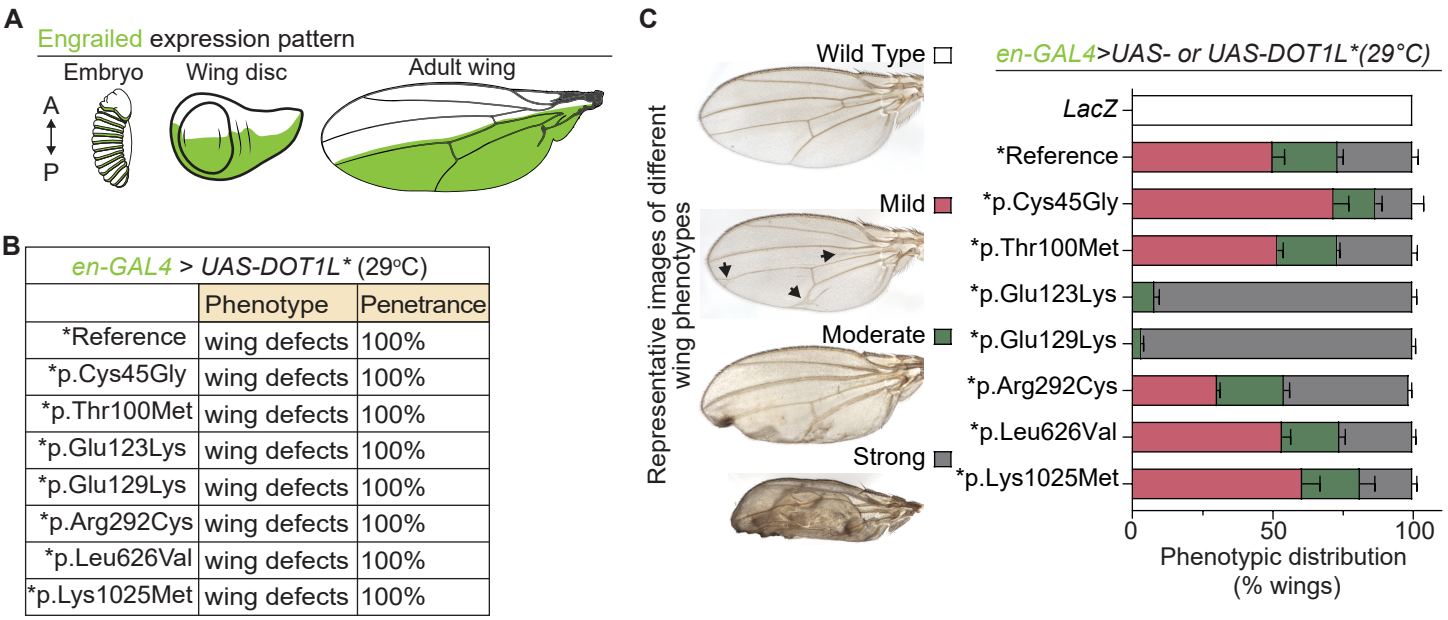

B

en-GAL4 > *UAS-DOT1L** (29°C)		
	Phenotype	Penetrance
*Reference	wing defects	100%
*p.Cys45Gly	wing defects	100%
*p.Thr100Met	wing defects	100%
*p.Glu123Lys	wing defects	100%
*p.Glu129Lys	wing defects	100%
*p.Arg292Cys	wing defects	100%
*p.Leu626Val	wing defects	100%
*p.Lys1025Met	wing defects	100%

Figure S5. Expression of reference or variant DOT1L in developing tissues causes wing deformities

(A) Schematic of engrailed expression from embryos to larval wing disc and adult wings.

(B) *en-GAL4 > UAS-DOT1L* reference or variant expressing flies show morphological wing defects such as whole wing blistering, necrosis, loss of cross-veins and extra vein branching.(en: engrailed)

(C) Representative images of different wing phenotypes (left panel) and the distribution of different wing phenotypes in *en-GAL4 > UAS-DOT1L* reference or variant expressing flies (right panel).

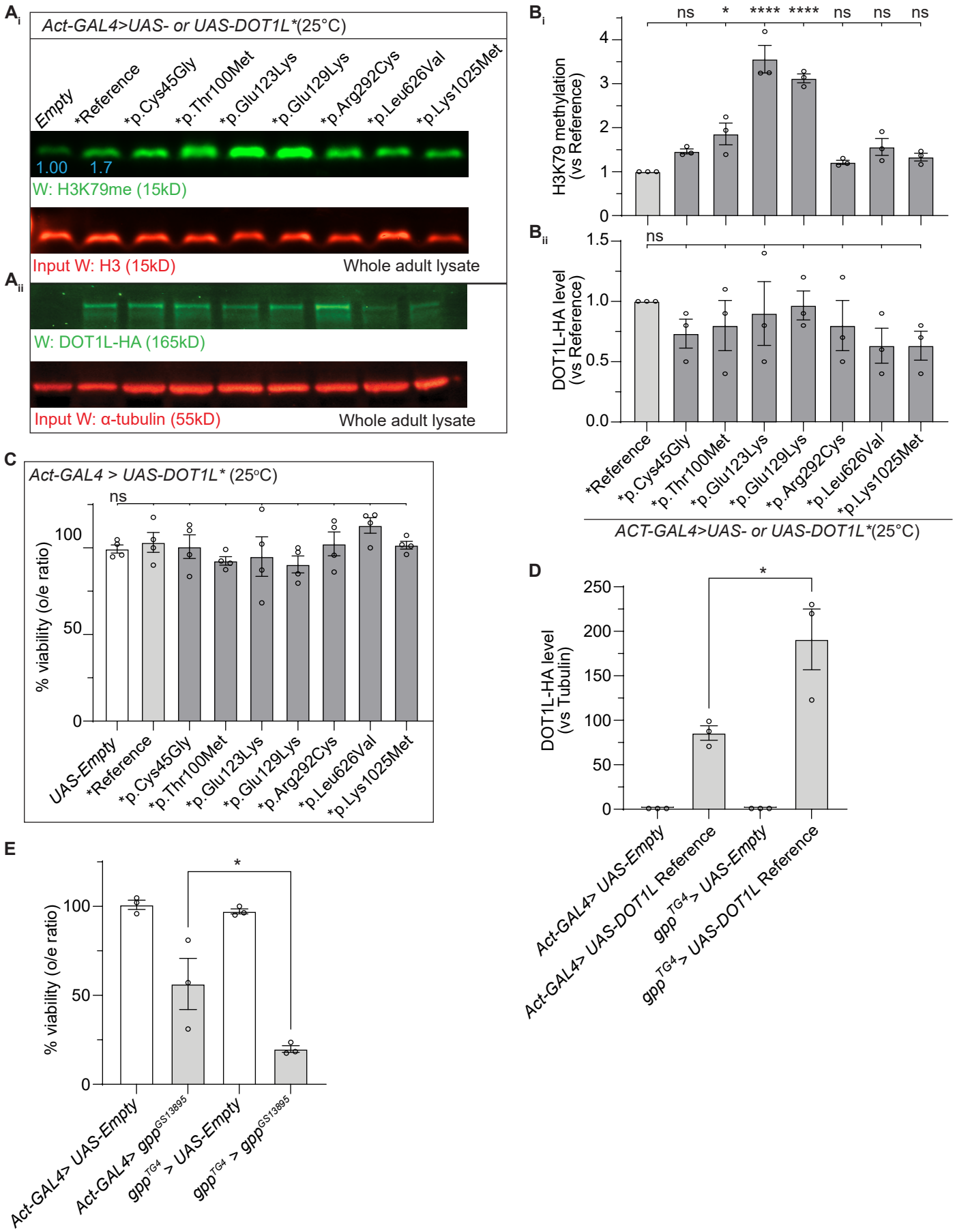
A
Act-GAL4>UAS- or UAS-DOT1L*(25°C)
Empty
*Reference
*p.Cys45Gly
*p.Thr100Met
*p.Glu123Lys
*p.Glu129Lys
*p.Arg292Cys
*p.Leu626Val
*p.Lys1025Met
1.00
1.7
W: H3K79me (15kD)
Input W: H3 (15kD)
Whole adult lysate
A
W: DOT1L-HA (165kD)
Input W: α-tubulin (55kD)
Whole adult lysate
B
H3K79 methylation (vs Reference)
ns
*
****
****
ns
ns
ns
B
DOT1L-HA level (vs Reference)
ns
*Reference
*p.Cys45Gly
*p.Thr100Met
*p.Glu123Lys
*p.Glu129Lys
*p.Arg292Cys
*p.Leu626Val
*p.Lys1025Met
ACT-GAL4>UAS- or UAS-DOT1L*(25°C)
C
Act-GAL4 > UAS-DOT1L* (25°C)
ns
% viability (o/e ratio)
UAS-Empty
*Reference
*p.Cys45Gly
*p.Thr100Met
*p.Glu123Lys
*p.Glu129Lys
*p.Arg292Cys
*p.Leu626Val
*p.Lys1025Met
D
*
DOT1L-HA level (vs Tubulin)
Act-GAL4> UAS-Empty
Act-GAL4> UAS-DOT1L Reference
gpp TG4 > UAS-Empty
gpp TG4 > UAS-DOT1L Reference
E
*
% viability (o/e ratio)
Act-GAL4> UAS-Empty
Act-GAL4> gppGS13895
gppTG4 > UAS-Empty
gppTG4 > gppGS13895

Figure S6. H3K79 methylation pattern of flies ubiquitously expressing human DOT1L and variants

(A_i) H3K79 methylation levels and (A_{ii}) DOT1L levels in flies ubiquitously expressing reference or variant *DOT1L* cDNAs. Flies expressing reference *DOT1L* show increased H3K79 methylation compared to control flies (*Act-GAL4* > *UAS-Empty*). Protein lysate from 10 adult flies were prepared for each sample. H3K79 methylation levels were normalized with loading control, H3, and fold change for each sample were calculated by comparing normalized H3K79 methylation levels to reference *DOT1L* expressing flies. DOT1L levels were normalized with loading control, α-tubulin, and fold change for each sample were calculated by comparing normalized DOT1L levels to reference *DOT1L* expressing flies. All the crosses were performed at 25^{o}C. Blue numbers indicate the fold change of H3K79 methylation level in reference when compared to control (*UAS-Empty*).

(B_i) Normalized H3K79 methylation band intensities for each group from three independent experiments were plotted as mean ± SEM, and statistical significance was determined by one-way ANOVA for multiple groups (* $p<0.05$, **** $p < 0.0001$). (B_{ii}) Normalized DOT1L band intensities for each group from three independent experiments were plotted as mean ± SEM, and statistical significance was determined by one-way ANOVA for multiple groups.

(C) Percent viability of flies ubiquitously (*Act-GAL4*) expressing reference or variant *DOT1L* cDNAs. All the crosses were performed at 25^{o}C. Percent viabilities (o/e ratios) from three independent experiments were plotted as mean ± SEM, and statistical significance was determined by one-way ANOVA for multiple groups.

(D) Expression of DOT1L cDNA in gpp expression domains using gppTG4 results in higher protein levels than ubiquitous expression of DOT1L using Act-GAL4 driver. Normalized DOT1L band intensities for control (UAS-empty) and UAS-DOT1L-Reference from three independent experiments (Figure 4E and Figure S6A) were plotted as mean ± SEM, and statistical significance was determined by one-way ANOVA for multiple groups.

(E) Percent viability of flies expressing fly gpp (gppGS13895) ubiquitously (Act-GAL4) or in gpp expression domains (gppTG4). All the crosses were performed at 25oC. Percent viabilities (o/e ratios) from three independent experiments were plotted as mean ± SEM, and statistical significance was determined by one-way ANOVA for multiple groups (* $p<0.05$).

Table S2. Details on match outcomes from Genematcher for *DOT1L* from October 2017 to June 2019

Event Type	Date of Match	Country of Clinician/Individual	Outcome	Variant	Sample Provided for DNAm Profiling
Original individual	N/A	Canada	Included in study	c.133T>G, p.Cys45Gly	Yes*
Previously published	N/A	England	Included in study	c.874C>T, p.Arg292Cys	Yes
Match	October 17th 2017	Netherlands	No response	-	-
Match	October 17th 2017	Netherlands	No response	-	-
Match	October 17th, 2017	France	No response	-	-
Match	October 17th, 2017	USA	Included in study	c.299C>T, p.Thr100Met	Yes
Match	December 5th, 2017	USA	No response after initial contact	[frameshift variant]	-
Match	December 19th, 2017	USA	Included in study	c.1352A>G, p.Asp451Gly	Yes (for both family members)
Match	March 19th, 2018	USA	Included in study	c.367G>A, p.Glu123Lys	Yes
Match	May 7th, 2018	France	Included in study	c.385G>A, p.Glu129Lys	Yes
Match	May 7th, 2018	France	Included in study	c.3074A>T, p.Lys1025Met	Yes*
Match	July 18th, 2018	New Zealand	Included in study	c.367G>A, p.Glu123Lys	No (not available; individual deceased)
Match	June 11th 2019	Norway	Included in study	c.1876C>G, p.Leu626Val	Yes

*not utilized in analysis due to lack of age matched controls

Table S3. Sequencing methods for individuals with *DOT1L* variants

Proband	1	2	3 NZ	4 Ch	5 OR	6	7	8	9	10	11
***DOT1L* variant (NM-032482.3)**	c.133T>G p.Cys45Gly	c.299C>T p.Thr100Met	c.367G>A p.Glu123Lys	c.367G>A p.Glu123Lys	c.367G>A p.Glu123Lys	c.385G>A p.Glu129Lys	c.1876C>G p.Leu626Val	c.2557C>T p.Arg853Cys	c.3074A>T p.Lys1025Met	c.874C>T p.Arg292Cys	c.1352A>G p.Asp451Gly
Sequencing approach	Trio genome sequencing	Trio genome sequencing	Singleton exome sequencing	Whole exome sequencing	Trio exome sequencing	Trio exome sequencing	Trio exome sequencing	Whole exome sequencing	Trio exome sequencing	Trio exome sequencing	Trio exome sequencing
Capture reagent	-	N/A	SOPHiA Genetics Clinical Exome Solution v1	N/A	GeneDx Proprietary System	Roche SeqCap EZ MedExome	Nextera Rapid Capture Exome Kit (Illumina)	N/A	Roche SeqCap EZ MedExome	SureSelect RNA baits (Agilent)	N/A
Sequencer	HiSeq X platform (Illumina Inc)	HiSeq X platform (Illumina Inc)	Illumina Inc	N/A	Illumina Inc	Illumina NextSeq 500	NextSeq 500 (Illumina)	N/A	Illumina NextSeq 500	Illumina HiSeq	N/A
Location of Sequencing	The Center for Applied Genomics, Toronto, Canada	HudsonAlpha Clinical Services Lab, Huntsville, Alabama	SOPHiA GENETICS	N/A	GeneDx	Genetic laboratory, Pitié-Salpêtrière Hospital, Paris, France	Telemark Hospital Trust, Skien, Norway	N/A	Genetic laboratory, Pitié-Salpêtrière Hospital, Paris, France	Genetics services of the UK National Health Service and the Republic of Ireland	N/A
Publication of Sequencing Methods	PMID: 32960281	-	-	-	-	PMID: 31580924	PMID: 26534809	-	PMID: 31580924	PMID: 28135719	-

Table S4. Publicly available fly lines used in this study

Fly Line	Genotype	BDSC #
gpp^{XXV}	*In(3R)gppXXV, gppXXV/TM3, P{ActGFP}JMR2, Ser1*	42231
Deficiency	*w[1118]; Df(3R)BSC193/TM6B, Tb[+]*	9620
Genomic rescue	*w[1118]; Dp(3;2)GV-CH321-05H03, PBac{y[+mDint2] w[+mC]=GV-CH321-05H03}VK00037/CyO*	90095
gpp RNAi #1	*y1 v1; P{TRiP.JF01284}attP2*	31327
gpp RNAi #2	*y1 v1; P{TRiP.JF01283}attP2/TM3, Ser1*	31481
gpp RNAi #3	*y[1] sc[*] v[1] sev[21]; P{y[+t7.7] v[+t1.8]=TRiP.GL01325}attP2*	41893
gpp RNAi #4	*y[1] v[1]; P{y[+t7.7] v[+t1.8]=TRiP.HMJ02129}attP40*	42556
Luciferase RNAi	*y[1] v[1];; P{y[+t7.7] v[+t1.8]=TRiP.JF01355}attP2*	31603
ey-GAL4 (on II)	*w[*]; P{w[+m*] =GAL4-ey.H}3-8*	5534
da-GAL4 (on III)	*w[*]; P{w[+mW.hs]=GAL4-da.G32}UH1, Sb[1]/TM6B, Tb[1]*	55851
en-GAL4 (on II)	*w[1118]; P{w[+mW.hs]=en2.4-GAL4}e16E, P{w[+mC]=UAS-RFP.W}2/CyO*	30557
act-GAL4 (on II)	*y[1] w[*]; P{w[+mC]=Act5C-GAL4}25FO1/CyO, y[+]*	4414
repo-GAL4 (on III)	*w[1118]; P{w[+m*]=GAL4}repo/TM3, Sb[1]*	7415
UAS-mCherry. NLS (on II)	*w[*]; P{w[+mC]=UAS-mCherry.NLS}2; MKRS/TM6B, Tb[1]*	38425
UAS-Empty (on II)	*w[*]; P{w[+mC]=UAS}/CyO*	
gpp^{GS13895}	*y[1] w[67c23]; P{w[+mC]=GSV6}GS13895/TM3, Sb[1] Ser[1]*	Kyoto 205608

Table S5. Mutagenesis and qPCR primers used in this study

Name	Assay	Forward primer (5'-3')	Reverse primer (5'-3')
p.Cys45Gly	Mutagenesis	CCGATGGGTCgGTGAAGAAATC	ATGGTCTCGATGATTTCATG
p.Thr100Met	Mutagenesis	AAGCTGAACAtGCGGCCGTCC	CATGGGCTGCGTGGTGCC
p.Glu123Lys	Mutagenesis	GACCGACCCCaAGAAGCTCAA	ACCGAGTGGTTGTAGACC
p.Glu129Lys	Mutagenesis	CAACAACTACaAGCCCTTCTCCCC	AGCTTCTCGGGGTCGGTC
p.Arg292Cys	Mutagenesis	CACCATCATGtGCGTGGTGGAGC	CCGATGTCACTCAAGTTTC
p.Leu626Val	Mutagenesis	GAAGCAGGCCgTGAAGAGCCA	TCCTTCAACAGCTTCTCCAG
p.Lys1025Met	Mutagenesis	GAGGCCAGCAtGGGAGACCTGCCC	GGGCAACGGGCCCTGGGC
qPrimer1	qPCR	ATCGTTGCATTGGAAAAAGG	GTACGGCGGCATTGTAAACT
qPrimer2	qPCR	CCATTGGAAGGTCTAGCAGC	CTGCTGCACGTCGTTGAC
RpL32	qPCR	TAAGCTGTCGCACAAATGGCG	AACGCGGTTCTGCATGAGCA

Table S7. Clinical features of individuals with suspected non-diagnostic variants in *DOT1L*

Individual	10	11
***DOT1L* variant (NM_032482.3)**	c.874C>T p.Arg292Cys	c.1352A>G p.Asp451Gly
Inheritance	*de novo*	Inherited from unaffected father
Sex	Female	Female
Age at last assessment	11 years	11 months
Medical History		
Brain anomalies (MRI/ CT)	N/A	N/A
Cardiac Anomalies	No	No
Hypotonia	No	No
Musculoskeletal anomalies	No	Yes Torticollis flexible hips, leg length discrepancy, right sided weakness with facial asymmetry
Urogenital anomalies	No	No
Hearing loss	No	Yes
Ophthalmological anomalies	No	Yes Amblyopia, anisometropia
Growth and Development		
Global developmental delay	Yes	-
Intellectual Disability	Yes	-
Language	Non-verbal	Speech delay, articulation concern
Height percentile	27.8%	3.3%
Microcephaly (percentile)	No (10^{th})	No (63^{rd})

Abbreviations are as follows: N/A: Not available

Table S8. Summary of variant details, allele frequencies and *in-silico* predictions for all *DOT1L* variants reported in our study

Variant Details									
Type	Missense	Missense	Missense	Missense	Missense	Missense	Missense	Missense	Missense
g. coordinates [GRCh37 (Chr19)]	g.2185861T>G	g.2191045C>T	g.2191113G>A	g.2191131G>A	g.2207590C>T	g.2211098A>G	g.2214548C>G	g.2217783C>T	g.2222242A>T
c. variant (NM_032482.3)	c.133T>G	c.299C>T	c.367G>A	c.385G>A	c.874C>T	c.1352A>G	c.1876C>G	c.2557C>T	c.3074A>T
p. variant (NP_115871.1)	p.Cys45Gly	p.Thr100Met	p.Glu123Lys	p.Glu129Lys	p.Arg292Cys	p.Asp451Gly	p.Leu626Val	p.Arg853Cys	p.Lys1025Met
Variant Allele Frequencies (searched December 2022)									
gnomAD v2.1.1	0	0	0	0	0	31	0	0	1
gnomAD v3.1.2	0	0	0	0	0	19	0	0	0
TOPMed Bravo	0	0	0	0	0	1	0	2	0
deCAF	0	2	0	0	0	97	0	0	0
***In Silico* Predictions & Conservation Metrics**									
Aggregated Prediction (Franklin)	Deleterious (0.71)	Benign (0.12)	Uncertain (0.55)	Uncertain (0.55)	Uncertain (0.36)	Benign (0.09)	Uncertain (0.29)	Uncertain (0.41)	Benign (0.07)
Revel	Deleterious (Supporting) (0.67)	Benign (Moderate) (0.12)	Uncertain (0.47)	Uncertain (0.47)	Benign (Supporting) (0.24)	Benign (Moderate) (0.09)	Benign (Moderate) (0.17)	Uncertain (0.31)	Benign (Moderate) (0.07)
Varity	Deleterious (0.96)	Deleterious (low) (0.43)	Deleterious (0.84)	Deleterious (0.72)	Deleterious (0.64)	Benign (0.08)	Benign (low) (0.28)	Deleterious (low) (0.44)	Benign (low) (0.25)
MutationAssessor	Low deleterious probability (1.83)	Medium deleterious probability (1.94)	Medium deleterious probability (1.98)	Medium deleterious probability (1.99)	Medium deleterious probability (2.09)	Medium deleterious probability (2.05)	Medium deleterious probability (1.96)	Medium deleterious probability (2.33)	Medium deleterious probability (1.98)
FATHMM	Uncertain (1.93)	Uncertain (2.06)	Uncertain (2.02)	Uncertain (2.05)	Uncertain (1.95)	Uncertain (1.81)	Uncertain (1.5)	Uncertain (1.39)	Uncertain (1.68)

MetaLR	Benign (low) (0.15)	Benign (0.13)	Benign (0.11)	Benign (0.11)	Benign (0.05)	Benign (low) (0.25)	Benign (low) (0.17)	Benign (low) (0.17)	Benign (0.15)
BayesDel	Uncertain (0.09)	Benign (Supporting) (-0.35)	Uncertain (-0.11)	Uncertain (-0.14)	Uncertain (-0.06)	Benign (Moderate) (-0.43)	Benign (Supporting) (-0.35)	Uncertain (-0.17)	Benign (Moderate) (-0.43)
CADD	Phred: 27.0 Raw score: 3.912343	Phred: 25.4 Raw score: 3.620297	Phred: 29.2 Raw score: 4.170345	Phred: 26.0 Raw score: 3.745109	Phred: 24.7 Raw score: 3.406433	Phred: 25.6 Raw score: 3.652334	Phred: 23.8 Raw score: 3.080506	Phred: 24.8 Raw score: 3.453433	Phred: 23.0 Raw score: 2.738641
Metadome	Tolerance score (dn/ds): 0.07 (highly intolerant)	Tolerance score (dn/ds): 0.4 (intolerant)	Tolerance score (dn/ds): 0.06 (highly intolerant)	Tolerance score (dn/ds): 0.06 (highly intolerant)	Tolerance score (dn/ds): 0.12 (highly intolerant)	Tolerance score (dn/ds): 0.62 (slightly intolerant)	Tolerance score (dn/ds): 0.34 (intolerant)	Tolerance score (dn/ds): 0.58 (slightly intolerant)	Tolerance score (dn/ds): 0.62 (slightly intolerant)
Grantham distance	Large physicochemical difference (159)	Moderate physicochemical difference (81)	Small physicochemical difference (56)	Small physicochemical difference (56)	Large physicochemical difference (180)	Moderate physicochemical difference (94)	Small physicochemical difference (32)	Large physicochemical difference (180)	Moderate physicochemical difference (95)
GERP	Uncertain (4.68)	Uncertain (4.75)	Uncertain (4.75)	Uncertain (4.75)	Uncertain (3.63)	Uncertain (3.62)	Uncertain (3.96)	Uncertain (4.15)	Uncertain (3.49)
Amino acid residue conservation (13 species)	Highly conserved (11/13)	Moderately conserved (8/13)	Highly conserved (11/13)	Highly conserved (11/13)	Moderately conserved (10/13)	Moderately conserved (9/13)	Moderately conserved (10/13)	Moderately conserved (9/13)	Moderately conserved (8/13)
PhyloP	Moderately conserved nucleotide (7.08)	Moderately conserved nucleotide (5.64)	Highly conserved nucleotide (9.17)	Highly conserved nucleotide (9.17)	Weakly conserved nucleotide (2.94)	Moderately conserved nucleotide (6.78)	Weakly conserved nucleotide (2.83)	Weakly conserved nucleotide (2.29)	Weakly conserved nucleotide (1.45)

Consortia

Undiagnosed Diseases Network

Maria T. Acosta, Margaret Adam, David R. Adams, Justin Alvey, Laura Amendola, Ashley Andrews, Euan A. Ashley, Mahshid S. Azamian, Carlos A. Bacino, Guney Bademci, Ashok Balasubramanyam, Dustin Baldridge, Jim Bale, Michael Bamshad, Deborah Barbouth, Pinar Bayrak-Toydemir, Anita Beck, Alan H. Beggs, Edward Behrens, Gill Bejerano, Hugo J. Bellen, Jimmy Bennet, Beverly Berg-Rood, Jonathan A. Bernstein, Gerard T. Berry, Anna Bican, Stephanie Bivona, Elizabeth Blue, John Bohnsack, Devon Bonner, Lorenzo Botto, Brenna Boyd, Lauren C. Briere, Elly Brokamp, Gabrielle Brown, Elizabeth A. Burke, Lindsay C. Burrage, Manish J. Butte, Peter Byers, William E. Byrd, John Carey, Olveen Carrasquillo, Thomas Cassini, Ta Chen Peter Chang, Sirisak Chanprasert, Hsiao-Tuan Chao, Gary D. Clark, Terra R. Coakley, Laurel A. Cobban, Joy D. Cogan, Matthew Coggins, F. Sessions Cole, Heather A. Colley, Cynthia M. Cooper, Heidi Cope, William J. Craigen, Andrew B. Crouse, Michael Cunningham, Precilla D'Souza, Hongzheng Dai, Surendra Dasari, Joie Davis, Jyoti G. Dayal, Matthew Deardorff, Esteban C. Dell'Angelica, Katrina Dipple, Daniel Doherty, Naghmeh Dorrani, Argenia L. Doss, Emilie D. Douine, Laura Duncan, Dawn Earl, David J. Eckstein, Lisa T. Emrick, Christine M. Eng, Cecilia Esteves, Marni Falk, Liliana Fernandez, Elizabeth L. Fieg, Paul G. Fisher, Brent L. Fogel, Irman Forghani, William A. Gahl, Ian Glass, Bernadette Gochuico, Rena A. Godfrey, Katie Golden-Grant, Madison P. Goldrich, Alana Grajewski, Irma Gutierrez, Don Hadley, Sihoun Hahn, Rizwan Hamid, Kelly Hassey, Nichole Hayes, Frances High, Anne Hing, Fuki M. Hisama, Ingrid A. Holm, Jason Hom, Martha Horike-Pyne, Alden Huang, Yong Huang, Wendy Introne, Rosario Isasi, Kosuke Izumi, Fariha Jamal, Gail P. Jarvik, Jeffrey Jarvik, Suman Jayadev, Orpa Jean-Marie, Vaidehi Jobanputra, Lefkothea Karaviti, Jennifer Kennedy, Shamika Ketkar, Dana Kiley, Gonench Kilich, Shilpa N. Kobren, Isaac S. Kohane, Jennefer N. Kohler, Deborah Krakow, Donna M. Krasnewich, Elijah Kravets, Susan Korrick, Mary Koziura, Seema R. Lalani, Byron Lam, Christina Lam, Grace L. LaMoure, Brendan C. Lanpher, Ian R. Lanza, Kimberly LeBlanc, Brendan H. Lee, Roy Levitt, Richard A. Lewis, Pengfei Liu, Xue Zhong Liu, Nicola Longo, Sandra K. Loo, Joseph Loscalzo, Richard L. Maas, Ellen F. Macnamara, Calum

A. MacRae, Valerie V. Maduro, Rachel Mahoney, Bryan C. Mak, May Christine V. Malicdan, Laura A. Mamounas, Teri A. Manolio, Rong Mao, Kenneth Maravilla, Ronit Marom, Gabor Marth, Beth A. Martin, Martin G. Martin, Julian A. Martínez-Agosto, Shruti Marwaha, Jacob McCauley, Allyn McConkie-Rosell, Alexa T. McCray, Elisabeth McGee, Heather Mefford, J. Lawrence Merritt, Matthew Might, Ghayda Mirzaa, Eva Morava, Paolo M. Moretti, Mariko Nakano-Okuno, Stan F. Nelson, John H. Newman, Sarah K. Nicholas, Deborah Nickerson, Shirley Nieves-Rodriguez, Donna Novacic, Devin Oglesbee, James P. Orengo, Laura Pace, Stephen Pak, J. Carl Pallais, Christina GS. Palmer, Jeanette C. Papp, Neil H. Parker, John A. Phillips III, Jennifer E. Posey, Lorraine Potocki, Barbara N. Pusey, Aaron Quinlan, Wendy Raskind, Archana N. Raja, Deepak A. Rao, Anna Raper, Genecee Renteria, Chloe M. Reuter, Lynette Rives, Amy K. Robertson, Lance H. Rodan, Jill A. Rosenfeld, Natalie Rosenwasser, Francis Rossignol, Maura Ruzhnikov, Ralph Sacco, Jacinda B. Sampson, Mario Saporta, Judy Schaechter, Timothy Schedl, Kelly Schoch, C. Ron Scott, Daryl A. Scott, Vandana Shashi, Jimann Shin, Edwin K. Silverman, Janet S. Sinsheimer, Kathy Sisco, Edward C. Smith, Kevin S. Smith, Emily Solem, Lilianna Solnica- Krezel, Ben Solomon, Rebecca C. Spillmann, Joan M. Stoler, Jennifer A. Sullivan, Kathleen Sullivan, Angela Sun, Shirley Sutton, David A. Sweetser, Virginia Sybert, Holly K. Tabor, Amelia L. M. Tan, Queenie K.-G. Tan, Mustafa Tekin, Fred Telischi, Willa Thorson, Cynthia J. Tifft, Camilo Toro, Alyssa A. Tran, Brianna M. Tucker, Tiina K. Urv, Adeline Vanderver, Matt Velinder, Dave Viskochil, Tiphanie P. Vogel, Colleen E. Wahl, Melissa Walker, Stephanie Wallace, Nicole M. Walley, Jennifer Wambach, Jijun Wan, Lee-kai Wang, Michael F. Wangler, Patricia A. Ward, Daniel Wegner, Monika Weisz-Hubshman, Mark Wener, Tara Wenger, Katherine Wesseling Perry, Monte Westerfield, Matthew T. Wheeler, Jordan Whitlock, Lynne A. Wolfe, Kim Worley, Changrui Xiao, Shinya Yamamoto, John Yang, Diane B. Zastrow, Zhe Zhang, Chunli Zhao, Stephan Zuchner

SUPPLEMENTARY REFERENCES

1. Liu, H., Liu, D.T., Lan, S., Yang, Y., Huang, J., Huang, J., and Fang, L. (2021). ASH1L mutation caused seizures and intellectual disability in twin sisters. J. Clin. Neurosci. 91, 69–74. 10.1016/J.JOCN.2021.06.038.
2. Kleefstra, T., Van Zelst-Stams, W.A., Nillesen, W.M., Cormier-Daire, V., Houge, G., Foulds, N., Van Dooren, M., Willemsen, M.H., Pfundt, R., Turner, A., et al. (2009). Further clinical and molecular delineation of the 9q subtelomeric deletion syndrome supports a major contribution of EHMT1 haploinsufficiency to the core phenotype. J. Med. Genet. 46, 598–606. 10.1136/jmg.2008.062950.
3. Goodman, S.J., Cytrynbaum, C., Chung, B.H.-Y., Chater-Diehl, E., Aziz, C., Turinsky, A.L., Kellam, B., Keller, M., Ko, J.M., Caluseriu, O., et al. (2020). EHMT1 pathogenic variants and 9q34.3 microdeletions share altered DNA methylation patterns in patients with Kleefstra syndrome. J. Transl. Genet. Genomics 4, 144–158. 10.20517/jtgg.2020.23.
4. Gibson, W.T., Hood, R.L., Zhan, S.H., Bulman, D.E., Fejes, A.P., Moore, R., Mungall, A.J., Eydoux, P., Babul-Hirji, R., An, J., et al. (2012). Mutations in EZH2 cause weaver syndrome. Am. J. Hum. Genet. 90, 110–118. 10.1016/j.ajhg.2011.11.018.
5. Choufani, S., Gibson, W.T., Turinsky, A.L., Chung, B.H.Y., Wang, T., Garg, K., Vitriolo, A., Cohen, A.S.A., Cyrus, S., Goodman, S., et al. (2020). DNA Methylation Signature for EZH2 Functionally Classifies Sequence Variants in Three PRC2 Complex Genes. Am. J. Hum. Genet. 106, 596–610. 10.1016/j.ajhg.2020.03.008.
6. Jones, W.D., Dafou, D., McEntagart, M., Woollard, W.J., Elmslie, F. V., Holder-Espinasse, M., Irving, M., Saggar, A.K., Smithson, S., Trembath, R.C., et al. (2012). De novo mutations in MLL cause Wiedemann-Steiner syndrome. Am. J. Hum. Genet. 91, 358–364. 10.1016/j.ajhg.2012.06.008.
7. Foroutan, A., Haghshenas, S., Bhai, P., Levy, M.A., Kerkhof, J., McConkey, H., Niceta, M., Ciolfi, A., Pedace, L., Miele, E., et al. (2022). Clinical Utility of a Unique Genome-Wide DNA Methylation Signature for KMT2A-Related Syndrome. Int. J. Mol. Sci. 23, 1815. 10.3390/ijms23031815.
8. Zech, M., Boesch, S., Maier, E.M., Borggraefe, I., Vill, K., Laccone, F., Pilshofer, V., Ceballos-Baumann, A., Alhaddad, B., Berutti, R., et al. (2016). Haploinsufficiency of KMT2B, Encoding the Lysine-Specific Histone Methyltransferase 2B, Results in Early-Onset Generalized Dystonia. Am. J. Hum. Genet. 99, 1377–1387. 10.1016/j.ajhg.2016.10.010.

9. Mirza-Schreiber, N., Zech, M., Wilson, R., Brunet, T., Wagner, M., Jech, R., Boesch, S., Škorvánek, M., Necpál, J., Weise, D., et al. (2022). Blood DNA methylation provides an accurate biomarker of KMT2B-related dystonia and predicts onset. Brain 145, 644–654. 10.1093/BRAIN/AWAB360.
10. Lee, S., Ochoa, E., Barwick, K., Cif, L., Rodger, F., Docquier, F., Pérez-Dueñas, B., Clark, G., Martin, E., Banka, S., et al. (2022). Comparison of methylation episignatures in KMT2B-and KMT2D-related human disorders. Epigenomics 14, 537–547. 10.2217/epi-2021-0521.
11. Cif, L., Demailly, D., Lin, J.P., Barwick, K.E., Sa, M., Abela, L., Malhotra, S., Chong, W.K., Steel, D., Sanchis-Juan, A., et al. (2020). KMT2B-related disorders: Expansion of the phenotypic spectrum and long-term efficacy of deep brain stimulation. Brain 143, 3242–3261. 10.1093/brain/awaa304.
12. Koemans, T.S., Kleefstra, T., Chubak, M.C., Stone, M.H., Reijnders, M.R.F., de Munnik, S., Willemsen, M.H., Fenckova, M., Stumpel, C.T.R.M., Bok, L.A., et al. (2017). Functional convergence of histone methyltransferases EHMT1 and KMT2C involved in intellectual disability and autism spectrum disorder. PLoS Genet. 13, e1006864. 10.1371/journal.pgen.1006864.
13. Cuvertino, S., Hartill, V., Colyer, A., Garner, T., Nair, N., Al-Gazali, L., Canham, N., Faundes, V., Flinter, F., Hertecant, J., et al. (2020). A restricted spectrum of missense KMT2D variants cause a multiple malformations disorder distinct from Kabuki syndrome. Genet. Med. 22, 980. 10.1038/s41436-020-0784-7.
14. Baldridge, D., Spillmann, R.C., Wegner, D.J., Wambach, J.A., White, F. V., Sisco, K., Toler, T.L., Dickson, P.I., Sessions Cole, F, et al. (2020). Phenotypic expansion of KMT2D-related disorder: Beyond Kabuki syndrome. Am J Med Genet A. 182(5):1053-1065. 10.1002/ajmg.a.61518.
15. Butcher, D.T., Cytrynbaum, C., Turinsky, A.L., Siu, M.T., Inbar-Feigenberg, M., Mendoza-Londono, R., Chitayat, D., Walker, S., Machado, J., Caluseriu, O., et al. (2017). CHARGE and Kabuki Syndromes: Gene-Specific DNA Methylation Signatures Identify Epigenetic Mechanisms Linking These Clinically Overlapping Conditions. Am. J. Hum. Genet. 100, 773–788. 10.1016/j.ajhg.2017.04.004.
16. Ng, S.B., Bigham, A.W., Buckingham, K.J., Hannibal, M.C., McMillin, M.J., Gildersleeve, H.I., Beck, A.E., Tabor, H.K., Cooper, G.M., Mefford, H.C., et al. (2010). Exome sequencing identifies MLL2 mutations as a cause of Kabuki syndrome. Nat. Genet. 42, 790–793. 10.1038/ng.646.

17. O'Donnell-Luria, A.H., Pais, L.S., Faundes, V., Wood, J.C., Sveden, A., Luria, V., Abou Jamra, R., Accogli, A., Amburgey, K., Anderlid, B.M., et al. (2019). Heterozygous Variants in KMT2E Cause a Spectrum of Neurodevelopmental Disorders and Epilepsy. Am. J. Hum. Genet. 104, 1210–1222. 10.1016/j.ajhg.2019.03.021.
18. Niihori, T., Ouchi-Uchiyama, M., Sasahara, Y., Kaneko, T., Hashii, Y., Irie, M., Sato, A., Saito-Nanjo, Y., Funayama, R., Nagashima, T., et al. (2015). Mutations in MECOM, Encoding Oncoprotein EVI1, Cause Radioulnar Synostosis with Amegakaryocytic Thrombocytopenia. Am. J. Hum. Genet. 97, 848–854. 10.1016/j.ajhg.2015.10.010.
19. Kurotaki, N., Imaizumi, K., Harada, N., Masuno, M., Kondoh, T., Nagai, T., Ohashi, H., Naritomi, K., Tsukahara, M., Makita, Y., et al. (2002). Haploinsufficiency of NSD1 causes Sotos syndrome. Nat. Genet. 30, 365–366. 10.1038/ng863.
20. Choufani, S., Cytrynbaum, C., Chung, B.H.Y., Turinsky, A.L., Grafodatskaya, D., Chen, Y.A., Cohen, A.S.A., Dupuis, L., Butcher, D.T., Siu, M.T., et al. (2015). NSD1 mutations generate a genome-wide DNA methylation signature. Nat. Commun. 2015 61 6, 1–7. 10.1038/ncomms10207.
21. Lozier, E.R., Konovalov, F.A., Kanivets, I. V., Pyankov, D. V., Koshkin, P.A., Baleva, L.S., Sipyagina, A.E., Yakusheva, E.N., Kuchina, A.E., and Korostelev, S.A. (2018). De novo nonsense mutation in WHSC1 (NSD2) in patient with intellectual disability and dysmorphic features. J. Hum. Genet. 63, 919–922. 10.1038/s10038-018-0464-5.
22. Kawai, T., Kinoshita, S., Takayama, Y., Onishi, E., Kamura, H., Kojima, K., Kikuchi, H., Terao, M., Sugawara, T., Migita, O., et al. (2023). DNA methylation signature in NSD2 loss-of-function variants appeared similar to that in Wolf-Hirschhorn syndrome. bioRxiv, 2023.01.06.522834. 10.1101/2023.01.06.522834.
23. Li, N., Subrahmanyan, L., Smith, E., Yu, X., Zaidi, S., Choi, M., Mane, S., Nelson-Williams, C., Bahjati, M., Kazemi, M., et al. (2016). Mutations in the Histone Modifier PRDM6 Are Associated with Isolated Nonsyndromic Patent Ductus Arteriosus. Am. J. Hum. Genet. 98, 1082–1091. 10.1016/j.ajhg.2016.03.022.
24. Arndt, A.K., Schafer, S., Drenckhahn, J.D., Sabeh, M.K., Plovie, E.R., Caliebe, A., Klopocki, E., Musso, G., Werdich, A.A., Kalwa, H., et al. (2013). Fine mapping of the 1p36 deletion syndrome identifies mutation of PRDM16 as a cause of cardiomyopathy. Am. J. Hum. Genet. 93, 67–77. 10.1016/j.ajhg.2013.05.015.
25. Yu, X., Yang, L., Li, J., Li, W., Li, D., Wang, R., Wu, K., Chen, W., Zhang, Y., Qiu, Z., et al. (2019). De Novo and Inherited SETD1A Variants in Early-onset Epilepsy. Neurosci. Bull. 35, 1045–1057. 10.1007/s12264-019-00400-w.

26. Kummeling, J., Stremmelaar, D.E., Raun, N., Reijnders, M.R.F., Willemsen, M.H., Ruiterkamp-Versteeg, M., Schepens, M., Man, C.C.O., Gilissen, C., Cho, M.T., et al. (2021). Characterization of SETD1A haploinsufficiency in humans and Drosophila defines a novel neurodevelopmental syndrome. Mol. Psychiatry 26, 2013–2024. 10.1038/s41380-020-0725-5.
27. Hiraide, T., Nakashima, M., Yamoto, K., Fukuda, T., Kato, M., Ikeda, H., Sugie, Y., Aoto, K., Kaname, T., Nakabayashi, K., et al. (2018). De novo variants in SETD1B are associated with intellectual disability, epilepsy and autism. Hum. Genet. 137, 95–104. 10.1007/s00439-017-1863-y.
28. Krzyzewska, I.M., Maas, S.M., Henneman, P., Lip, K. V.D., Venema, A., Baranano, K., Chassevent, A., Aref-Eshghi, E., Van Essen, A.J., Fukuda, T., et al. (2019). A genome-wide DNA methylation signature for SETD1B-related syndrome. Clin. Epigenetics 11, 1–15. 10.1186/S13148-019-0749-3/FIGURES/6.
29. Rabin, R., Radmanesh, A., Glass, I.A., Dobyns, W.B., Aldinger, K.A., Shieh, J.T., Romoser, S., Bombei, H., Dowsett, L., Trapane, P., et al. (2020). Genotype-phenotype correlation at codon 1740 of SETD2. Am. J. Med. Genet. A 182, 2037–2048. 10.1002/AJMG.A.61724.
30. Luscan, A., Laurendeau, I., Malan, V., Francannet, C., Odent, S., Giuliano, F., Lacombe, D., Touraine, R., Vidaud, M., Pasmant, E., et al. (2014). Mutations in SETD2 cause a novel overgrowth condition. J. Med. Genet. 51, 512–517. 10.1136/jmedgenet-2014-102402.
31. Lumish, H.S., Wynn, J., Devinsky, O., and Chung, W.K. (2015). Brief Report: SETD2 Mutation in a Child with Autism, Intellectual Disabilities and Epilepsy. J. Autism Dev. Disord. 45, 3764–3770. 10.1007/s10803-015-2484-8.